Proceedings of the 41st Polish Seminar on Positron Annihilation, Lublin, September 9–13, 2013

Positron Annihilation in $MnFe_2O_4$/MCM-41 Nanocomposite

M. Wiertel[a,*], Z. Surowiec[a], W. Gac[b] and M. Budzyński[a]

[a]Department of Nuclear Methods, Faculty of Mathematics, Physics and Computer Science
Maria Curie-Skłodowska University, pl. M. Curie-Skłodowskiej 1, 20-031 Lublin, Poland

[b]Department of Chemical Technology, Faculty of Chemistry, Maria Curie-Skłodowska University
pl. M. Curie-Skłodowskiej 3, 20-031 Lublin, Poland

In the paper results of studies of $MnFe_2O_4$/MCM-41 nanocomposites have been presented. The influence of manganese ferrite loading on changes of porous properties of mesoporous MCM-41 structure was studied by means of N_2 sorption/desorption method and positron annihilation lifetime spectroscopy. Disappearance of the longest-lived *ortho*-positronium component (τ_5) of pure MCM-41 mesoporous material in the positron annihilation lifetime spectra of $MnFe_2O_4$/MCM-41 measured in vacuum is a result of either *o*-Ps quenching or the Ps inhibition mechanism. Filling of pores in the studied nanocomposites by air at ambient pressure causes partial reappearance of the (τ_5) component except for the sample with maximum ferrite content. Both the (τ_5) component lifetime and intensity are suppressed together with increasing $MnFe_2O_4$ content by chemical quenching and inhibition of Ps formation occur. Observed anti-quenching effect of air is a result of two processes: neutralization of some surface active centres acting as inhibitors and considerably weaker paramagnetic quenching by O_2 molecules.

DOI: 10.12693/APhysPolA.125.793

PACS: 78.70.Bj, 34.80.Lx, 78.67.Bf, 62.23.Pq, 68.43.−h, 75.50.Gg, 78.47.D−

1. Introduction

A nanocomposite is a multiphase solid material where one of the phases has one, two or three dimensions of less than 100 nanometers (nm), or structures having nano--scale repeat distances between the different phases that make up the material [1]. Regarding synthesis route and an aim of production, a nanocomposite may be treated as a matrix to which nanoparticles have been added to improve or change a particular property of the material. Nanocomposites are attractive researching subject both from practical and theoretical point of view because of combination of special properties [2].

Magnetic manganese ferrite nanocomposites and similar to them can be used potentially as efficient adsorbents, catalysts [3] or baseline modified silica support for putting of specific chemical functional groups. Highly ordered mesoporous MCM-41 silica used as a support is characterized by uniform pore diameter distribution, large total pore volume and large specific surface area [4]. Free-volume structure in them is represented by primary pores along with specific vacancy-type defects within individual crystalline grains and intergranular boundaries. In any medium, the intrinsic lifetime of *ortho*--positronium (*o*-Ps) is reduced from 142 ns in vacuum by the process called pick-off annihilation. The *o*-Ps lifetime is dependent on the size of the pore in which the *o*-Ps atom is trapped. This gives a possibility to use *o*-Ps as a porosimetric probe to evaluate the average sizes in the approximate range from a few tenths of a nanometer to 100 nm. If the pores are partially or completely filled by some chemical species *o*-Ps living in localized states long enough can undergo various processes e.g. chemical reactions and *ortho-para* conversion. Relevant processes are called chemical quenching and paramagnetic quenching, respectively [5]. Chemical reactions with so-called inhibitors lead to inhibition of Ps formation and only have an effect on values of *o*-Ps lifetime components intensities. Chemical active centres scavenging electrons, positrons, holes etc. also act as inhibitors. All phenomena enumerated above may potentially give valuable information on the structural and chemical properties of micro- and mesoporous materials.

The aims of presented investigations was to give information about porosity structure and pores filling capacity of $MnFe_2O_4$/MCM-41 nanocomposites.

2. Experimental

The samples of $MnFe_2O_4$/MCM-41 nanocomposites with nominal Fe content equals to 5, 10, 20, and 40 wt% at constant molar relation Fe/Mn as 2:1 were obtained in two stages. First the mesoporous MCM-41 support was prepared. Next the appropriate portions of Fe and Mn from $Fe(NO_3)_3{\cdot}9H_2O$ and $Mn(C_2H_3O_2)_2{\cdot}4H_2O$ nitrate ethanol solutions were embedded into silica support by means of an incipient wetness impregnation method. The samples were initially dried at 100 °C and next calcined at 400 °C for 3 h. The relatively low calcinations temperature allows to obtain as small as possible ferrite particles dimensions with maximum dispersion in the support. From XRF results actual Fe contents were obtained, 4.3, 8.6, 17.2, and 35.2 wt%, respectively.

The porous structure of materials was analysed by the N_2 adsorption/desorption isotherms obtained volumetrically at 77 K. The adsorption data were used to evaluate the Brunauer–Emmett–Teller (BET) specific surface area, S_{BET}. The mesoporous structure was characterized by the distribution function of mesopore volume calculated by applying the Barrett–Joyner–Halenda (BJH) method [6].

*corresponding author; e-mail: marek.wiertel@umcs.pl

In PALS measurements the ^{22}Na positron source sealed in a kapton envelope was used. It was immersed between two about 2 mm thick layers of the powder sample, pressed together by a screwed cap inside a small copper container. This assembly was put in a vacuum chamber allowing to obtain pressure of the order of 5×10^{-4} Pa. Positron lifetime spectra were recorded at room temperature using a standard fast-slow coincidence spectrometer. In order to minimize effects of summing in the coincidence spectra so-called triangular geometry [7] was used. In this geometry the samples were shifted outside of a longitudinal axis of symmetry of two counter detecting system. At such a setting the resolution time was 0.27 ns (measured for ^{60}Co source with ^{22}Na windows set). The time base of the PALS setup was 1 μs. The total counts were not less than 10^8 for each spectrum measured in vacuum or in air. The positron lifetime spectra were analyzed using the LT program [8].

3. Results and discussion

The porous structure and surface properties of the MCM-41 matrix change significantly after incorporation of $MnFe_2O_4$ into this support. Manganese ferrite takes the form of nanoparticles and output material forms nanocomposite. Surface areas (S_{BET}) of nanocomposite samples with different ferrite content changing from about 565 m^2/g to 238 m^2/g, respectively (see inset in Fig. 1). These values are from twice to four times smaller than that for pure MCM-41 equals about 1100 m^2/g. The shape of the N_2 adsorption/desorption isotherms (type IV isotherm according to IUPAC classification [9]) shown in Fig. 2 for the samples (A), (B) and (C) (see Table) indicated the formation of regular mesopores with mean pore diameter (w_d) of about 2.9 nm. A small and flat hysteresis loop can be observed in the range of relative pressures ranging from 0.4 to 0.9 of relative pressure p/p_0 for the first three samples. This effect can indicate the presence of the same irregularities in the structure of silica mesoporous material, connected with slow development of bottle-ink type pores. The hysteresis loop for the $MnFe_2O_4$/MCM-41(D) (see Table) became big and steep which suggests an appearance of more open free volumes.

TABLE The lifetimes and intensities of o-Ps components measured in vacuum ($p \approx 5 \times 10^{-4}$ Pa) and in air for ferrite $MnFe_2O_4$/MCM-41 nanocomposites.

Sample		τ_3	τ_4	τ_5	I_3	I_4	I_5
		[ns]			[%]		
empty MCM-41	vacuum	3.46(38)	33.1(2.0)	124.92(80)	1.07(16)	0.88(33)	23.40(40)
	air	2.56(36)	17.84(88)	73.09(51)	1.36(21)	1.97(25)	18.36(37)
$MnFe_2O_4$/MCM-41(A)	vacuum	2.00(23)	10.54(51)	40.46(87)	6.01(44)	3.27(22)	2.50(24)
4.3 wt% Fe	air	2.23(24)	12.82(52)	65.50(68)	5.06(37)	3.23(20)	6.61(23)
$MnFe_2O_4$/MCM-41(B)	vacuum	1.56(18)	7.30(54)	26.95(87)	9.90(53)	1.98(21)	1.38(23)
8.6 wt% Fe	air	1.89(19)	9.98(47)	54.01(97)	7.70(47)	2.37(19)	1.93(17)
$MnFe_2O_4$/MCM-41(C)	vacuum	1.49(29)	6.74(79)	26.6(1.1)	4.11(56)	1.08(18)	0.92(24)
17.2 wt% Fe	air	2.34(29)	8.71(66)	36.9(1.1)	3.52(29)	1.57(23)	1.19(20)
$MnFe_2O_4$/MCM-41(D)	vacuum	1.06(30)	5.71(63)	26.2(1.3)	3.58(87)	0.70(17)	0.43(17)
35.2 wt% Fe	air	1.72(33)	7.08(71)	28.8(2.1)	1.63(32)	0.77(19)	0.19(18)

An increase of manganese ferrite loading induces distortion of the well-ordered MCM-41 structure and decrease of the total surface area of the samples. The typical for MCM-41 step on the isotherms at p/p_0 value of about 0.3 becomes less pronounced, and finally disappears for the (D) sample with the highest ferrite content. Such effects are most probably connected with formation of more and more bigger nanocrystallites and transformation of primary open pores into closed pores. In Fig. 1 pore sizes distributions (PSDs) calculated from the desorption isotherms by the BJH method are shown. In the table given in this figure average pore diameter values are given. In the PSD obtained for the sample (D) a relatively significant part stretching out up to a radius of the order of 50 nm appears. This part is related to pores significantly bigger than primary ones ($R_p \approx 1.5$ nm). Total BJH specific pore volumes after initial drop insignificantly increase for the last three samples (see Fig. 1).

In Fig. 3 five different PAL spectra for investigated samples measured in vacuum (bottom part) and in air at ambient pressure (top part) are presented. The intensities of the longest-lived component (τ_5) measured in air systematically decrease along with an increase of manganese ferrite content in the samples. Simultaneously rapid disappearance of this component can be observed in the measurements in vacuum (see Fig. 3). In fitting procedure it was assumed that they consist of five discrete exponential components. The first two are very short-lived, the former belonging in principle to the intrinsic decay of *para*-positronium (p-Ps, $\tau_1 \approx 0.13$ ns) and the latter which is related to the free positrons annihilation (e^+, $\tau_2 \approx 0.45$ ns). The (τ_2) component ori-

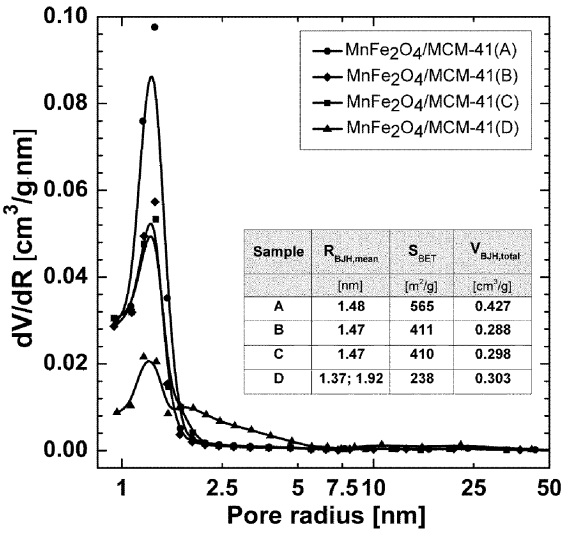

Sample	$R_{BJH,mean}$ [nm]	S_{BET} [m^2/g]	$V_{BJH,total}$ [cm^3/g]
A	1.48	565	0.427
B	1.47	411	0.288
C	1.47	410	0.298
D	1.37; 1.92	238	0.303

Fig. 1. Pore sizes distributions determined from N_2 adsorption/desorption isotherms of the investigated samples by BJH method. APD — average pore diameter obtained from adsorption.

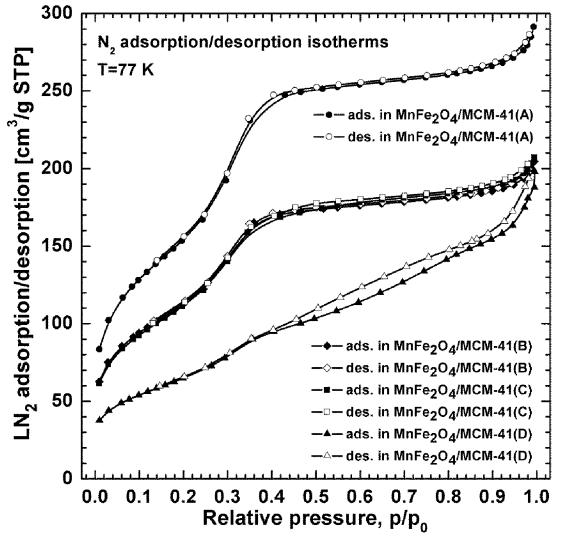

Fig. 2. Nitrogen adsorption/desorption isotherms for $MnFe_2O_4$/MCM-41 nanocomposites. For the sample labels explanation and Fe content see Table.

gins on the one hand from annihilation of free positrons trapped in vacancy clusters formed in ferrite nanoparticles or on their surfaces [10], on the other hand from positron annihilation in small structural open volumes in amorphous silica walls. As one can see these observed lifetimes are only mean values for several undistinguishable components comparable to the time resolution of the measuring system. The component's (τ_2) lifetime value remains almost constant but its intensity changes from about 40% in pure MCM-41 to about 90% in the sample (D) very similar for both series of measurements in vacuum and in air. It is simply related to the increasing number of manganese ferrite nanoparticles deposited mainly on surfaces of MCM-41 walls.

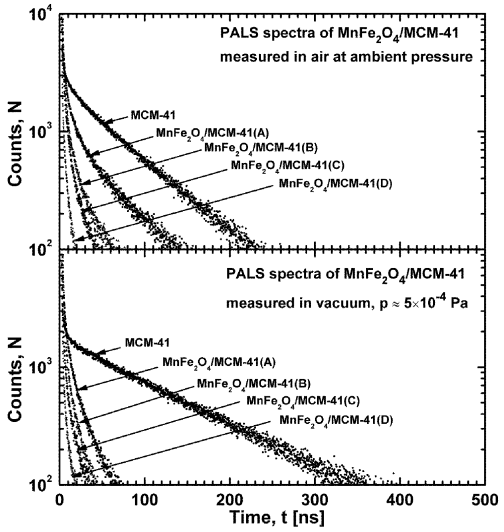

Fig. 3. Positron annihilation lifetime spectra of four $MnFe_2O_4$/MCM-41 samples measured in vacuum (a) and in air (b) normalized to time of measurement. Background is subtracted.

In contrary to the PALS results in nanocrystalline ferrites prepared by other method [11], in $FeMn_2O_4$/MCM-41 nanocomposite a bulk lifetime component of about 0.2 ns is not observed. In the papers [12] and [13] the results of investigations of similar $NiFe_2O_4(SiO_2)$ nanocomposites produced on the basis of amorphous silica by sol–gel method were reported. From PALS spectra analysis lifetime relating to positron free annihilation in the non-defective nanocrystalline grain volumes were derived. This lifetime is equal to about 0.14 ns. In the $MnFe_2O_4$/MCM-41 nanocomposites a component of lifetime in the same range was not found. It seems that in the ferrite nanocomposite samples obtained by the wetness impregnation route are defective in almost whole volume. Moreover, even $MnFe_2O_4$ nanoparticles located out of primary MCM-41 nanochannels do not aggregate into larger nanocrystallites.

In the investigated samples three long-lived o-Ps components were also observed in the positron lifetime spectra. Detailed values of lifetimes and intensities are given in Table. From the data obtained on intensities of o-Ps components it seems that I_2 increases mainly at the expense of the sum of intensities of all o-Ps components for the measurements performed in air and almost to the same extent at the expense of that sum and the first component intensity in the case of measurements in vacuum.

The shortest-lived o-Ps component (τ_3) is difficult to unique interpretation. It probably arises owing to the pick-off annihilation of o-Ps formed in the some kind of small open-type voids on surfaces of amorphous MCM-41 silica walls which are larger than those in which positrons

annihilate from free state. Components with lifetimes in the order of (1÷2) ns were observed in thin films of amorphous silica [14] and they were interpreted as belonging to o-Ps confined in voids of above mentioned type. The medium-lived one (τ_4) results from decay of o-Ps inside of silica nanochannels and the longest-lived among them (τ_5) is related to the pick-off annihilation of o-Ps trapped in free volume in intergranular spaces of the material [15].

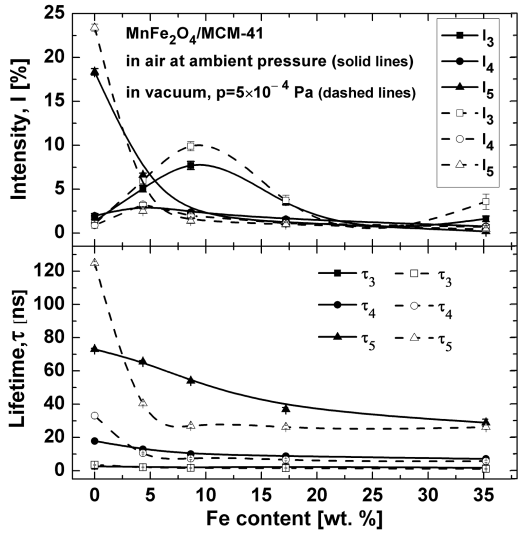

Fig. 4. The dependences of lifetimes (lower part) and intensities (upper part) of the positron free annihilation on Fe content for $MnFe_2O_4$/MCM-41 nanocomposites measured in air at ambient pressure and in vacuum, $p \approx 5 \times 10^{-4}$ Pa.

The o-Ps lifetimes and their intensities changes with increasing manganese ferrite content for the samples in air under ambient pressure are presented in Fig. 4. The lifetime τ_3 remains principally constant and τ_4 slightly decreases. According to our interpretation of these components origin these characters of dependences indicate that only inner spaces (pores) volumes somewhat lessen due to filling with ferrite In contrast to Fe-modified MCM-41 silica [16], in which Fe is incorporated into silica walls in the stage of MCM-41 making, also the (τ_5) lifetime for the manganese ferrite nanocomposite considerably decreases. As to intensities of the first two components, I_4 slightly decreases and I_3 exhibits maximum for the sample (B) both in vacuum and in air. The intensity of the last component rapidly falls in relation to that of pure MCM-41. It results from the lifetime and intensity changes observed for the fifth component that the both inhibition and quenching phenomena occur. Lifetime τ_5 observed in $MnFe_2O_4$/MCM-41(A) composite measured in air is about 10% smaller than the value observed for pure MCM-41 in air (Table) while analogous difference for measurement in vacuum for the same couple of samples is much larger. Differences in values of τ_5 for the last three samples measured in air related to the pure MCM-41 monotonically increases. In the case of measurements in vacuum the τ_5 values after a rapid drop remain almost constant for the samples (B), (C) and (D).

The difference between PALS spectra measured in vacuum and in air emerging as considerable larger intensity of the longest-lived component in the latter medium can be explained as follows. It is known that the adsorption of small amounts of the molecules on the pore surface increases the o-Ps lifetime, due to the blocking of active sites on the pore surface causing partial quenching of o-Ps [17]. In the case of the investigated samples probably a coating of $MnFe_2O_4$ deposits by monolayer of predominantly N_2 molecules from air takes place. The N_2 monolayer gives film thick enough to isolate semi-metallic manganese ferrite with much lower electron density layer. This kind of passivation of the manganese ferrite outweighs an effect of o-Ps quenching by an o-Ps to p-Ps conversion in interaction with paramagnetic air oxygen molecules.

At first glance it seems that there exist some discrepancies between pictures of porosity structure of the investigated samples obtained from N_2 adsorption/desorption measurements and by means of PALS method. The most important one is related to the primary pore sizes. These obtained from BJH method remain practically unchanged for the first three samples whereas monotonically decreasing τ_4 values suggest their decrease. The reason of that is probably caused by chemical quenching on which the N_2 adsorption/desorption method is not sensitive. Moreover, in the PALS spectra for the sample (D) none additional positron lifetime component with a lifetime value close to τ_4 was not revealed while in PSD distribution for the same sample a broad peak with maximum at 1.92 nm is present.

4. Conclusions

Information of $MnFe_2O_4$/MCM-41 mesoporous structure changes obtained from N_2 A/D measurements seems to be partially inconsistent to PALS results, which is at least partially a natural consequence of considerable dissimilarity of the used methods. The use of PALS method to determine of pore sizes in such complex material is impossible in a direct way. An interpretation of results is made difficult because of strong influence of disturbing factors such as chemical quenching and inhibitions on long-lived components parameters. The adsorption of air molecules on the ferrite nanoparticles prevents chemical quenching and inhibition of the o-Ps formation effects. The obtained from PALS measurements data are result of competition of two phenomena: practically switching off a pick-off mechanism related to interaction of o-Ps with chemical species occurring in $MnFe_2O_4$/MCM-41 nanocomposite and considerably weaker paramagnetic quenching by oxygen molecules.

References

[1] P.M. Ajayan, in: *Nanocomposite Science and Technology*, Eds. P.M. Ajayan, L.S. Schadler, P.V. Braun, Wiley-VCH, Weinheim 2003.

[2] J. Mohapatra, A. Mitra, D. Bahadur, M. Aslam, *Cryst. Eng. Commun.* **15**, 524 (2013).

[3] B. Sahoo, S.K. Sahu, S. Nayak, D. Dhara, P. Pramanik, *Catal. Sci. Technol.* **2**, 1367 (2012).

[4] J.S. Beck, J.C. Vartuli, W.J. Roth, M.E. Leonowicz, C.T. Kresge, K.D. Schmitt, C.T.W. Chu, D.H. Olson, E.W. Sheppard, S.B. McCullen, J.B. Higgins, J.L. Schlenker, *J. Am. Chem. Soc.* **114**, 10834 (1992).

[5] D.M. Schrader, Y.C. Jean, in: *Positron and Positronium Chemistry*, Eds. D.M. Schrader, Y.C. Jean, Elsevier, Amsterdam 1988, p. 1.

[6] E.P. Barrett, L.G. Joyner, P.P. Halenda, *J. Am. Chem. Soc.* **73**, 373 (1951).

[7] T. Goworek, W. Górniak, J. Wawryszczuk, *Nucl. Instrum. Methods Phys. Res. A* **321**, 560 (1992).

[8] J. Kansy, *Nucl. Instrum. Methods Phys. Res. A* **374**, 235 (1996).

[9] J. Rouquerol, D. Avnir, C.W. Fairbridge, D.H. Everett, J.H. Haynes, N. Pernicone, J.D.F. Ramsay, K.S.W. Sing, K.K. Unger, *Pure Appl. Chem.* **66**, 1739 (1994).

[10] S. Chakrabarti, S. Chaudhuri, P.M.G. Nambissan, *Phys. Rev. B* **71**, 064105 (2005).

[11] S. Bandyopadhyay, A. Roy, D. Das, S.S. Ghugrea, J. Ghose, *Philos. Mag.* **83**, 765 (2003).

[12] S. Mitra, K. Mandal, S. Sinha, P.M.G. Nambissan, S. Kumar, *J. Phys. D: Appl. Phys.* **39**, 4228 (2006).

[13] S. Chakraverty, S. Mitra, K. Mandal, P.M.G. Nambissan, S. Chattopadhyay, *Phys. Rev. B* **71**, 024115 (2005).

[14] S. Dannefaer, T. Bretagnon, D. Kerr, *J. Appl. Phys.* **74**, 884 (1993).

[15] Y. Kobayashi, K. Ito, T. Oka, K. Hirata, *Radiat. Phys. Chem.* **76**, 224 (2007).

[16] M. Wiertel, Z. Surowiec, M. Budzyński, W. Gac, *Nukleonika* **58**, 245 (2013).

[17] S.Y. Chuang, S.J. Tao, *J. Chem. Phys.* **54**, 4902 (1971).